

Wave packet dynamics of entangled two-mode states

C. Sudheesh, S. Lakshmibala, and V. Balakrishnan*

Department of Physics, Indian Institute of Technology Madras, Chennai 600 036, India

Abstract

We consider a model Hamiltonian describing the interaction of a single-mode radiation field with the atoms of a nonlinear medium, and study the dynamics of entanglement for specific non-entangled initial states of interest: namely, those in which the field mode is initially in a Fock state, a coherent state, or a photon-added coherent state. The counterparts of near-revivals and fractional revivals are shown to be clearly identifiable in the entropy of entanglement. The “overlap fidelity” of the system is another such indicator, and its behaviour corroborates that of the entropy of entanglement in the vicinity of near-revivals. The expectation values and higher moments of suitable quadrature variables are also examined, with reference to possible squeezing and higher-order squeezing.

PACS numbers: 42.50.-p, 03.67.Mn, 42.50.Dv, 42.50.Md

arXiv:quant-ph/0603020v1 2 Mar 2006

*Electronic address: sudheesh,slbala,vbalki@physics.iitm.ac.in

I. INTRODUCTION

A problem of considerable interest in quantum dynamics is that of the identification of signatures of non-classical effects in the temporal behaviour of quantum mechanical expectation values in nonlinear systems. The dynamics of a quantum wave packet governed by a nonlinear Hamiltonian provides adequate scope for such an investigation to be carried out, as a wide variety of non-classical effects such as revivals and fractional revivals [1], as well as squeezing, are displayed by the wave packet as it evolves in time.

While a generic initial wave packet $|\psi(0)\rangle$ governed by a nonlinear Hamiltonian spreads rapidly during its evolution, it could return to its original state (apart from an overall phase) at multiples of a revival time T_{rev} , under certain conditions. This is signalled by the return of the overlap $C(t) = |\langle\psi(0)|\psi(t)\rangle|^2$ to its initial value of unity at $t = nT_{\text{rev}}$. Further, at specific instants of time in between two successive revivals, fractional revivals of the wave packet may occur. This is characterised by the splitting up of the initial wave packet into a number of spatially distributed sub-packets, each of which is similar to the original wave packet. Both revivals and fractional revivals of a wave packet arise due to very specific quantum interference properties between the basis states comprising the original wave packet [2].

It is evident that, at exact revivals of any initial state, quantum mechanical expectation values of observables return to their initial values. Distinctive signatures of different fractional revivals show up in the time dependence of the higher moments of appropriate operators. By tracking the time evolution of various moments of certain operators, selective identification of different fractional revivals can be achieved [3]. Since the initial state of the system turns out to play a crucial role in determining its subsequent dynamics and the non-classical features it exhibits, these signatures also help assess the degree of coherence of the initial state [4]. Further, it has been shown that the squeezing and higher-order squeezing properties of certain quadrature variables in the neighbourhood of a fractional revival of the wave packet provide quantifiable measures of the departure from perfect coherence of the initial state [5]. The studies in Refs. [3]-[5] have been carried out in the context of the propagation of a single-mode electromagnetic field in a Kerr-like medium, modelled by the Hamiltonian $H = \hbar\chi a^{\dagger 2}a^2$, where a , a^{\dagger} are photon annihilation and creation operators, and $\chi (> 0)$ represents the susceptibility of the nonlinear medium. (We shall refer to this as the case of “single-mode” dynamics in what follows.) The initial state of the field has been

taken to be a member of the family of photon-added coherent states [6], as the properties of such states include a quantifiable degree of departure from perfect coherence, sub-Poisson statistics (a standard deviation that is asymptotically proportional to a power of the mean that is less than $\frac{1}{2}$), and phase-squeezing. The standard oscillator coherent state (CS) is a limiting case of a photon-added coherent state (PACS).

A similar investigation of the dynamics of two interacting modes is of special interest, in view of an additional phenomenon that occurs in this case—namely, entanglement. Interesting aspects of the entanglement that arises when an initial single-mode coherent state passes through a nonlinear medium modelled by the above-mentioned Hamiltonian, followed by an interaction with a 50% beam splitter, have been discussed by van Enk [7]. Sanz *et al.* [8] have examined the non-classical effects that arise in the dynamics of two entangled modes governed by a nonlinear Hamiltonian, in the framework of an exactly solvable case: two modes of an electromagnetic field interacting in a Kerr-like medium. Taking the initial state to be a direct product, either of two Fock states or of two coherent states, the periodic exact revival of these states has been established, and the manner in which these properties are mirrored in the collapse and revival phenomena displayed by the expectation values of appropriate observables has been investigated. The collapses are marked by expectation values remaining constant over a certain interval, while the revivals are signalled by rapid pulsed variations of the expectation values. These features are the close analogues of those displayed in the single-mode case mentioned earlier. It must be noted, however, that the specific Hamiltonian considered in these studies is symmetric in the two modes, with identical nonlinear terms and a symmetric coupling between the modes. As a consequence, the Hamiltonian is readily diagonalised, and the resultant dynamics displays a considerable degree of regularity, including the occurrence of revivals.

However, this symmetry is not expected to be present in a generic Hamiltonian governing the interaction of a single-mode field with a nonlinear medium. The best one can hope for is the occurrence of approximate or *near*-revivals for most values of the parameters in the Hamiltonian. In addition to near-revivals and related phenomena, several other features of interest are exhibited in general by the dynamics of two interacting modes. Our objective in this paper is to demonstrate and investigate these. We will also examine the link between the extent to which revivals occur and the nature of the initial state. A suitable Hamiltonian for our purposes is the one [9] that describes the interaction of a single-mode field with

the atoms of the nonlinear medium through which it propagates. The latter is modelled by an anharmonic oscillator. The important point to note is that this Hamiltonian is not symmetric in the two interacting degrees of freedom, and, moreover, is not diagonalisable in general.

In order to bring out the salient features of entanglement dynamics, we consider initial states that are direct products of the field and atom modes. Entanglement of these two modes sets in during temporal evolution. However, for certain ranges of values of the parameters and coupling constants in the governing Hamiltonian, we show that the modes disentangle at specific instants during the evolution, and the state of the system returns close to its initial form (apart from a phase). This feature is clearly the analogue of wave packet revivals in the dynamics of a single mode. Appropriate indicators to determine quantitatively the extent and nature of near-revivals and their fractional counterparts are the entanglement entropies, as measured by the sub-system von Neumann entropy (SVNE) and the sub-system linear entropy (SLE), the sub-system considered here being the field mode. These entropies show marked dips at near-revivals, and are also seen to reduce significantly in certain cases at fractions $\frac{1}{2}$, $\frac{1}{3}$, $\frac{2}{3}$ and $\frac{1}{4}$ of the near-revival time T_{rev} , signalling the appearance of counterparts of fractional revivals. We have also examined the behaviour of another indicator of near-revivals, the ‘‘overlap fidelity’’ $C(T_{\text{rev}})$, as a function of a relevant parameter in the Hamiltonian, namely, the coupling between the sub-systems represented by the two modes. This fidelity is defined as the maximum value that the overlap $|\langle \psi(0) | \psi(t) \rangle|^2$ attains in the vicinity of the first near-revival, for a given initial state. We study the role of the specific (non-entangled) initial state considered, and the extent of departure of the initial field mode from coherence, on the subsequent revival properties of the state. In particular, the link between the entanglement of states and their squeezing properties has been investigated. The initial state of the field mode is taken to be a member of the family of photon-added coherent states. The advantages of a PACS have already been stated. We add that this family of states is now within the realm of experimental realisation in the foreseeable future, a single-photon added coherent state having recently been generated experimentally and characterised using quantum tomography[10]. With increasing departure from coherence of the initial field mode, the entropy of entanglement at any instant during the temporal evolution of the quantum state of the system also increases, and even near-revivals do not occur.

The plan of the rest of this paper is as follows: In Section II, we discuss the relevant features of the model Hamiltonian [9] we use to study the dynamics of two-mode entanglement. In Section III, we examine three different indicators or measures of the extent to which a state revives at any instant: the first of these comprises the instantaneous SVNE and SLE. The trends observed here are corroborated by the behaviour of the overlap fidelity, which we examine as a function of the strength of the coupling between the field and the medium. Finally, certain operators whose expectation values carry signatures of the different fractional revivals are also identified. We have examined the dynamics of several initial states, taking the atom to be in the ground state while the field is, respectively, in a Fock state, a CS, and a PACS. This enables us to analyse systematically the effects of different initial field modes on the dynamics. The relationship between the squeezing property of the state of the system and the initial field mode is also brought out.

II. SINGLE-MODE FIELD IN A NONLINEAR MEDIUM

The interaction of a single-mode field of frequency ω with the atoms of the nonlinear medium through which it propagates is modelled by the Hamiltonian[9]

$$H = \omega a^\dagger a + \omega_0 b^\dagger b + \gamma b^{\dagger 2} b^2 + g(a^\dagger b + b^\dagger a). \quad (1)$$

(We have set $\hbar = 1$.) a and a^\dagger are the annihilation and creation operators pertaining to the field, while b and b^\dagger are the corresponding atom operators. The medium is modelled by an anharmonic oscillator with frequency ω_0 and anharmonicity parameter γ . The coupling constant g is a measure of the strength of the coupling between the field mode and the atom mode. It is easily verified that the total number operator $N_{\text{tot}} = a^\dagger a + b^\dagger b$ commutes with H . We reiterate that the foregoing Hamiltonian is not symmetric in the two modes, even when $\omega = \omega_0$.

The Fock basis is given by $\{|n'\rangle_a \otimes |n\rangle_b\}$, where n' and n are the eigenvalues of $a^\dagger a$ and $b^\dagger b$, respectively. In the absence of the coupling constant g , H is trivially a direct sum of Hamiltonians that are functions of the number operators for the two modes. In the absence of the anharmonicity parameter γ , the coupled Hamiltonian is essentially linear in each of the sub-system variables, and can be diagonalised in terms of linear combinations of the original ladder operators. In physical terms, this leads to fairly simple dynamics, essentially entailing

a simple periodic exchange of energy between the two sub-systems or modes. When both g and γ are non-zero, the system displays a wide variety of dynamical behaviour, depending on the value of the ratio γ/g . Additional insight into the nature of the model Hamiltonian is gained by re-expressing it in terms of angular momentum operators defined in the usual manner, according to $J_+ = a^\dagger b$, $J_- = ab^\dagger$, $J_z = \frac{1}{2}(a^\dagger a - b^\dagger b)$. We then have

$$H = \hbar \left[\frac{1}{2}(\omega + \omega_0 - \gamma)\mathbf{N}_{\text{tot}} + (\omega - \omega_0 + \gamma)J_z + \frac{1}{4}\gamma(\mathbf{N}_{\text{tot}} - 2J_z)^2 + 2gJ_x \right], \quad (2)$$

where $\mathbf{N}_{\text{tot}}(\mathbf{N}_{\text{tot}} + 2) = 4J^2$. As $[\mathbf{N}_{\text{tot}}, H] = 0$, we may write the basis states as $|N - n\rangle_a \otimes |n\rangle_b$, using N to label the eigenvalues of \mathbf{N}_{tot} . For notational simplicity, let us write

$$|N - n\rangle_a \otimes |n\rangle_b \equiv |N - n; n\rangle. \quad (3)$$

It is evident that $\langle N - n; n | H | N' - n'; n' \rangle = 0$, if $N \neq N'$. Hence, for each given value of N , the Hamiltonian H can be diagonalised in the space of the states $|N - n; n\rangle$, where $n = 0, 1, \dots, N$. Let the eigenvalues and eigenstates of H be λ_{Ns} and $|\psi_{Ns}\rangle$, respectively, where $s = 0, 1, \dots, N$ for a given N , and $N = 0, 1, \dots$ *ad inf*. It is convenient to expand $|\psi_{Ns}\rangle$ in the basis $\{|N - n; n\rangle\}$ as

$$|\psi_{Ns}\rangle = \sum_{n=0}^N d_n^{Ns} |N - n; n\rangle, \quad d_n^{Ns} = \langle N - n; n | \psi_{Ns} \rangle. \quad (4)$$

In this basis, (each block of) H can be represented as a real, symmetric, tridiagonal matrix. Its eigenvalues λ_{Ns} and eigenstates $|\psi_{Ns}\rangle$ can be found numerically using appropriate matrix algebra routines [11, 12]. An initial state $|\psi(0)\rangle$ of the system evolves in time to the state

$$|\psi(t)\rangle = U(t) |\psi(0)\rangle = \sum_{N=0}^{\infty} \sum_{s=0}^N \exp(-i\lambda_{Ns}t) \langle \psi_{Ns} | \psi(0) \rangle |\psi_{Ns}\rangle \quad (5)$$

at time t . For our purposes, it is necessary to compute the time-dependent density operator $\rho(t)$ for different choices of the initial state $|\psi(0)\rangle$, as well as the reduced density matrices corresponding to the field and atom sub-systems. The main steps in the procedure are outlined in the Appendix.

As already mentioned, if either g or γ is equal to zero, the Hamiltonian in Eq. (1) is exactly solvable, and there is periodic exchange of energy between the field and atom oscillators. For non-zero values of the ratio γ/g of the respective strengths of the nonlinearity and the field-atom interaction, collapses and near-revivals could occur over certain intervals of time, in

between these periodic exchanges of energy. This phenomenon translates into the behaviour of expectation values of certain observables as well. For instance, during a collapse of the energy exchange over an interval of time, the mean photon number $\langle a^\dagger a \rangle$ remains essentially constant. A revival of the energy exchange is signalled by rapid oscillations of the mean photon number about this value, over the relevant time interval.

Further, when the atomic oscillator is initially in its ground state, while the field starts either in a Fock state or in a coherent state, one finds the following results[9]: (a) For weak nonlinearity ($\gamma/g \ll 1$), collapses and revivals of the mean photon number occur almost periodically in time, for both kinds of initial field states. The near-revival time is approximately given by $2\pi/\gamma$ in the former case, and $4\pi/\gamma$ in the latter [13]. (When γ is *exactly* equal to zero, there is no nonlinearity in H , and the system is merely periodic. There is no question of revivals in this case.) (b) For $\gamma/g \sim 1$, such collapses and revivals occur more irregularly if the field is initially in a coherent state, compared to the case when it is initially in a Fock state. As the nonlinearity is increased ($\gamma/g \gg 1$), collapses and revivals gradually become less discernible. Bearing these results in mind, in the next section we examine the manner in which the above-mentioned collapse and revival phenomena are mirrored in the entropy of entanglement of the system. We identify suitable observables which carry signatures of collapses and revivals, and discuss the influence of the departure from coherence of the initial state of the field on the extent to which it revives subsequently.

III. ENTANGLEMENT PROPERTIES

We now examine the detailed dynamics of three different initial states which are direct products of the field and atom states, evolving under the Hamiltonian in Eq. (1). As stated earlier, the initial state of the atom is taken to be the oscillator ground state $|0\rangle_b$, while that of the field is, respectively, (a) a Fock state $|n'\rangle_a$, $n' = 0, 1, \dots$; (b) a CS $|\alpha\rangle_a$; and (c) an m -photon-added CS $|\alpha, m\rangle_a$, $m = 1, 2, \dots$. (Recall that the suffixes a and b correspond to the electromagnetic field and the atoms of the medium, respectively.) The CS and PACS referred to have the standard expansions in the Fock basis, namely,

$$|\alpha\rangle = e^{-|\alpha|^2/2} \sum_{l=0}^{\infty} \frac{\alpha^l}{\sqrt{l!}} |l\rangle \quad (6)$$

and

$$|\alpha, m\rangle = \frac{(a^\dagger)^m |\alpha\rangle}{\sqrt{\langle \alpha | a^m a^{\dagger m} | \alpha \rangle}} = \frac{(a^\dagger)^m |\alpha\rangle}{\sqrt{m! L_m(-\nu)}}, \quad (7)$$

where $\alpha \in \mathbb{C}$, $\nu = |\alpha|^2$, and L_m is the Laguerre polynomial of order m .

As we are dealing with a pure bipartite system, it is natural to consider the time-dependences of S_k , the sub-system von Neumann entropy (SVNE), and δ_k , the sub-system linear entropy (SLE), where the suffix k stands for either a or b , depending on the sub-system considered. These quantities are defined as

$$S_k(t) = -\text{Tr}_k \{ \rho_k(t) \ln \rho_k(t) \} \quad (8)$$

and

$$\delta_k(t) = 1 - \text{Tr}_k \{ \rho_k^2(t) \}, \quad (9)$$

where $\rho_k(t)$ is the time-dependent reduced density operator for the sub-system concerned. In terms of the set of eigenvalues of $\rho_k(t)$, we have

$$S_k(t) = - \sum_i \lambda_k^{(i)}(t) \ln \lambda_k^{(i)}(t), \quad \delta_k(t) = 1 - \sum_i \{ \lambda_k^{(i)}(t) \}^2, \quad (10)$$

where the summation runs over all the eigenvalues $\lambda_k^{(i)}(t)$.

Our objective is to investigate the detailed dynamics of entangled states [14] exhibiting revival phenomena. We therefore restrict ourselves here to the case of weak nonlinearity, i. e., $\gamma/g \ll 1$, as this is the situation in which these phenomena occur most unambiguously. For illustrative purposes, we set the values of the parameters at $\omega = \omega_0 = 1$, and $\gamma = 1$, $g = 100$, so that $\gamma/g = 10^{-2}$. As stated in the preceding section, some of the steps involved in the calculation of the foregoing sub-system entropies are given in the Appendix. For pure states in a bipartite system, of course, $S_a = S_b$ and $\delta_a = \delta_b$ at any instant of time. Figures 1(a) and (b) depict plots of SVNE and SLE versus gt for respective initial states $|10\rangle_a \otimes |0\rangle_b$ (or $|10; 0\rangle$, in our notation) and $|\alpha\rangle_a \otimes |0\rangle_b \equiv |\alpha; 0\rangle$ with the parameter value $\nu = 1$. The band-like appearance of the plots in Fig. 1(a) arises from the extremely rapid oscillations of the ordinates. The corresponding plots for an initial state $|\alpha, 5\rangle_a \otimes |0\rangle_b \equiv |(\alpha, 5); 0\rangle$ in the cases $\nu = 1$ and $\nu = 5$ are shown in Figs. 2(a) and (b) respectively. In all the cases above, the SVNE (the upper plot in each figure) is larger than the SLE (the lower plot in each figure) at any instant of time. It is evident that both SVNE and SLE display roughly similar oscillatory behaviour in time. However, certain striking differences arise in the time

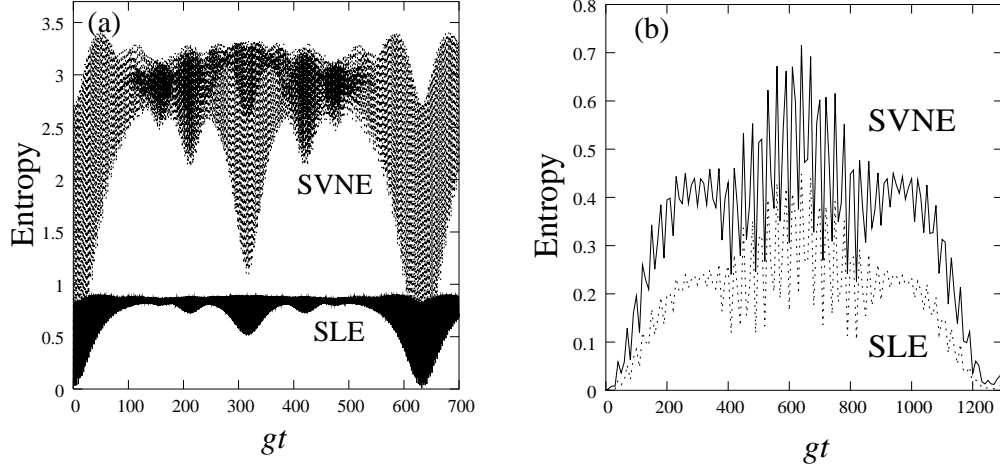


FIG. 1: SVNE and SLE *vs.* gt with $\gamma/g = 10^{-2}$ for (a) an initial Fock state $|10; 0\rangle$ and (b) an initial coherent state $|\alpha; 0\rangle$ with $\nu = 1$.

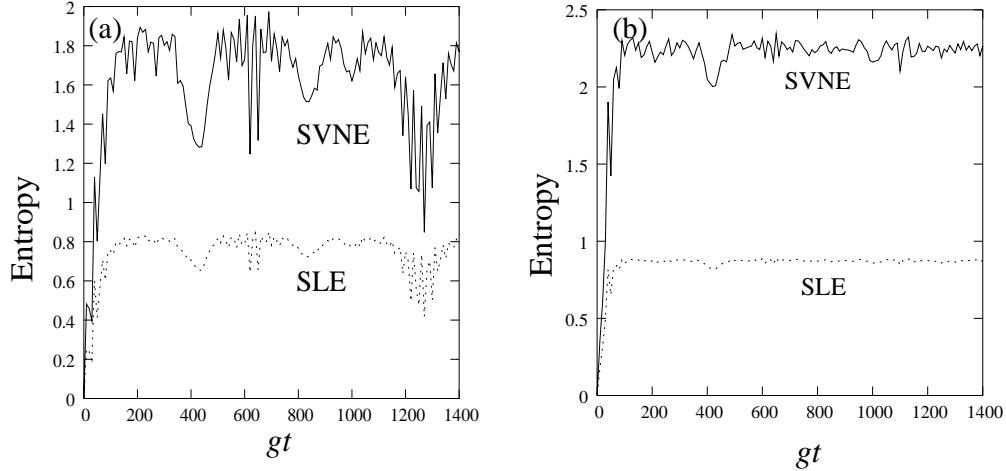


FIG. 2: SVNE and SLE *vs.* gt for an initial state $|(\alpha, 5); 0\rangle$ for (a) $\nu = 1$ and (b) $\nu = 5$ ($\gamma/g = 10^{-2}$).

evolution of the SVNE and SLE, depending on the actual initial state considered. If the field is initially in a Fock state or a CS, the entropies return to values close to zero at regular intervals of time (see Fig. 1), signalling a near-revival of the initial state. (Note that the revival times are indeed approximately equal to 2π and 4π , respectively, recalling that we have set $\gamma = 1$ and $g = 100$.) In contrast, if the initial state of the field is a PACS, the extent of revival is considerably reduced (see Figs. 2(a) and (b)). Further, with an increase

in the value of ν , the oscillations in the SVNE and SLE die down. This effect is enhanced for larger values of m , as seen in the rapid increase and saturation of both the SVNE and SLE for an initial state $|(\alpha, 5); 0\rangle$ for $\nu = 5$, in contrast to the corresponding plots for $\nu = 1$.

It is also clear that the SVNE and SLE display marked oscillatory behaviour near $\frac{1}{2}T_{\text{rev}}$, $\frac{1}{3}T_{\text{rev}}$ and $\frac{1}{4}T_{\text{rev}}$. This behaviour may be regarded as the counterpart, in our coupled system, of the fractional revivals seen in the case of a single-mode nonlinear Hamiltonian [3, 4]. Again, these oscillations die down in amplitude with increasing m when the initial state of the field is a PACS, and are most pronounced if the field is initially in a Fock state.

As mentioned in Section 1, another indicator that characterises the degree of revival of an initial state is the overlap fidelity, defined as

$$C(T_{\text{rev}}) = \max_{t \sim T_{\text{rev}}} |\langle \psi(0) | \psi(t) \rangle|^2, \quad (11)$$

which is the maximum value attained by the overlap function in the vicinity of the first near-revival time corresponding to a given initial state $|\psi(0)\rangle$. In Figs. 3(a) and (b), we have plotted this quantity as a function of g , the strength of the coupling between the field and atom modes, again for non-entangled initial states in which the field is in a CS or a PACS. We see quantitatively how, with an increase in the departure from coherence of the initial field state, near-revivals occur only for ever increasing values of the coupling strength g relative to the coefficient γ of the nonlinearity in the Hamiltonian.

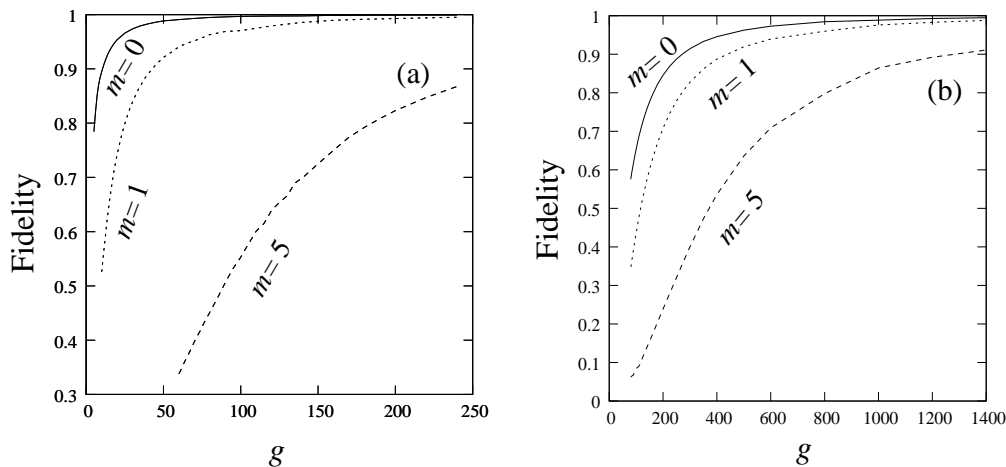


FIG. 3: Overlap fidelity *vs.* g for an initial state $|(\alpha, m); 0\rangle$, with $\gamma = 1$ and (a) $\nu = 1$ and (b) $\nu = 5$.

Next, we consider whether signatures of the features seen above appear in the time evolution of expectation values of observables. For this purpose, we define the quadratures

$$\xi = (x_a + x_b)/2, \quad \eta = (p_a + p_b)/2, \quad (12)$$

where

$$x_a = (a + a^\dagger)/\sqrt{2}, \quad x_b = (b + b^\dagger)/\sqrt{2} \quad (13)$$

and

$$p_a = (a - a^\dagger)/(i\sqrt{2}), \quad p_b = (b - b^\dagger)/(i\sqrt{2}). \quad (14)$$

If the field is initially in a Fock state, both $\langle \xi \rangle$ and $\langle \eta \rangle$ vanish identically at all times. Setting

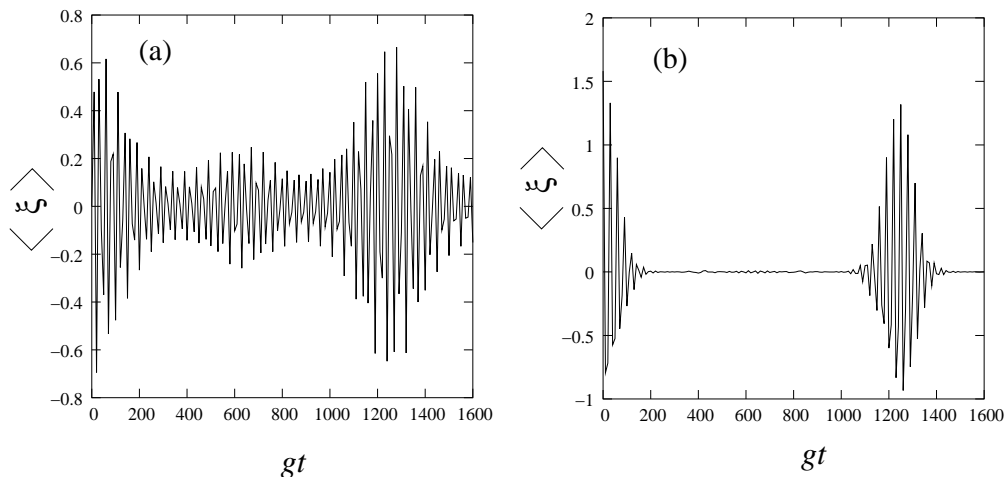


FIG. 4: $\langle \xi \rangle$ vs. gt for an initial state $|\alpha; 0\rangle$ with $\nu = 1$ and $\nu = 5$, respectively ($\gamma/g = 10^{-2}$).

$\omega = \omega_0 = 1$, $\gamma = 1$ and $g = 100$ as before (for ready comparison with the time evolution of the SVNE and SLE discussed above), we have plotted $\langle \xi \rangle$ versus gt for an initial state $|\alpha; 0\rangle$ with $\nu = 1$ and 5 , respectively, in Figs. 4(a) and (b). Figure 4(a) shows that $\langle \xi \rangle$ displays rapid pulsed oscillations near $t = 4\pi$, similar to its behaviour near $t = 0$. This manifestation of revivals is consistent with the behaviour of the SVNE and SLE in this case, *cf.* Fig. 1(b). The collapses are not sharp, in the sense that $\langle \xi \rangle$ is not constant over the time interval between successive revivals—oscillatory bursts occur in between, with a slight enhancement of these oscillations around the fractional revival at $\frac{1}{2}T_{\text{rev}}$. In contrast, the collapses in between revivals are much more complete for larger values of ν , as seen in Fig. 4(b), consistent with the corresponding behaviour of the SVNE and SLE in this case. An

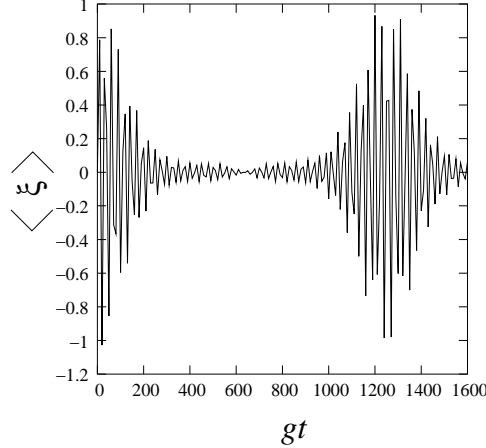


FIG. 5: $\langle \xi \rangle$ vs. gt for an initial state $|(\alpha, 1); 0\rangle$ with $\nu = 1$ ($\gamma/g = 10^{-2}$).

interesting feature is that these collapses become much sharper for even a marginal departure from coherence of the initial state of the field (i. e., even for as low a value as $m = 1$). $\langle \xi \rangle$ remains virtually constant over the duration of the collapse, and then bursts into rapid oscillations close to revivals, as seen in Fig. 5 which corresponds to $m = 1$ and $\nu = 1$. As in the case of single-mode dynamics, the amplitude of the oscillations in the neighbourhood of T_{rev} decreases significantly with an increase in m . Thus, for small values of ν , it is easy to distinguish between an initial CS and an initial PACS. The expectation value of η also displays these signatures. We may add that, while the sub-system variables x_a , x_b , p_a and p_b do exhibit near-revivals in their expectation values, their higher moments do not capture the occurrence of fractional revivals. However, the higher moments of the combinations ξ and η do carry distinguishing signatures to selectively pin-point the analogues of the different fractional revivals that occur in the single-mode case. Hence ξ and η are the appropriate dynamical variables in the interacting system under consideration.

The standard deviation $\Delta\xi$ of ξ reflects the occurrence of the dips in the plots of the SVNE and SLE at $\frac{1}{2}T_{\text{rev}}$. The plot of $\Delta\xi$ versus gt for an initial state $|10; 0\rangle$ shows a burst of rapid oscillations at $t \simeq \pi$ (Fig. 6). This feature holds for an initial CS or PACS as well, as is evident (Fig. 7) from the sudden burst of oscillations in $\Delta\xi$ around $t \simeq 2\pi$ for initial states $|\alpha; 0\rangle$, $|(\alpha, 1); 0\rangle$ and $|(\alpha, 5); 0\rangle$ (recall that $T_{\text{rev}} \simeq 4\pi$ in this case).

We note that *squeezing* occurs in the neighbourhood of $\frac{1}{2}T_{\text{rev}}$ when the initial state of the field is a coherent state: $\Delta\xi$ drops below the value $\frac{1}{2}$ (the horizontal dotted line in Fig. 7)

in the case when the initial state is $|\alpha; 0\rangle$, in contrast to what happens for an initial PACS $|(\alpha, m); 0\rangle$. While this is similar to the squeezing property seen in the case of single-mode dynamics, such parallels do not hold in the case of higher-order squeezing. The relevant quadrature variables in this case are obvious generalisations of those considered in the case of single-mode dynamics [15], and are given by [16]

$$Z_1 = \frac{(a^q + a^{\dagger q} + b^q + b^{\dagger q})}{2\sqrt{2}}, \quad Z_2 = \frac{(a^q - a^{\dagger q} + b^q - b^{\dagger q})}{2i\sqrt{2}}. \quad (15)$$

In contrast to the single-mode example, even for weak nonlinearity ($\gamma/g = 10^{-2}$) and $\nu = 1$, amplitude-squared squeezing ($q = 2$) is absent at $t = \frac{1}{2}T_{\text{rev}}$ whether the field is in a Fock state, or a CS, or a PACS.

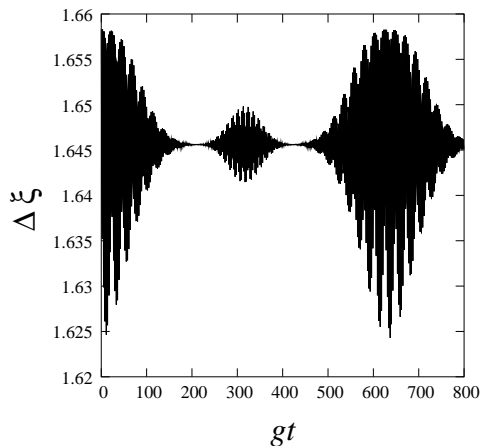


FIG. 6: $\Delta\xi$ vs. gt for an initial state $|10; 0\rangle$ ($\gamma/g = 10^{-2}$).

Finally, turning to the higher moments of ξ and η , we note that all odd moments of ξ vanish identically for all t if the initial state is a direct product of Fock states. For small values of ν , the higher moments of ξ show distinct signatures at fractional revivals only if m is sufficiently large. However, for larger values of ν , such signatures appear even in the case of an initial CS ($m = 0$). In contrast to this, the temporal evolution of the variances and higher moments of the subsystem variables x_a , x_b , p_a and p_b do not display these signatures. In this sense, the expectation values of sub-system quadrature variables would seem to be inappropriate choices for investigating collapse and revival phenomena in the presence of entanglement, although, as we have shown, the sub-system entropies are eminently suitable indicators in this regard.

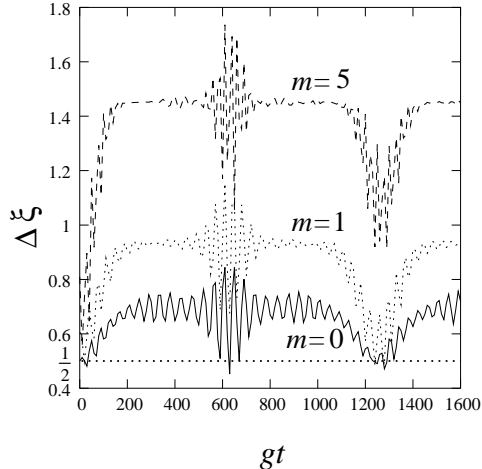


FIG. 7: $\Delta\xi$ vs. gt for an initial state $|(\alpha, m); 0\rangle$ with $\nu = 1$ and $m = 0, 1$ and 5 , respectively ($\gamma/g = 10^{-2}$).

The model Hamiltonian we have used to study two-mode dynamics leads to several other interesting features that are manifested in the expectation values of sub-system variables, as the parameters in H are varied. In particular, the ergodicity properties of the system, in a “phase space” spanned by such expectation values, exhibit a range of behaviour from quasi-periodicity to exponential instability—the latter, notwithstanding the fact that the classical counterpart of H is an integrable two-freedom Hamiltonian. These results will be reported elsewhere.

Acknowledgments

This work was supported in part by the Department of Science and Technology, India, under Project No. SP/S2/K-14/2000.

APPENDIX: CALCULATION OF THE DENSITY MATRIX

We outline here the procedure used for calculating the density matrix elements required for the determination of the entropies and related quantities in the main text.

From Eq. (5) for the state vector of the system at time t , it follows that the time-

dependent density matrix $\rho(t)$ is

$$\rho(t) = \sum_{N=0}^{\infty} \sum_{s=0}^N \sum_{N'=0}^{\infty} \sum_{s'=0}^{N'} \exp[-i(\lambda_{Ns} - \lambda_{N's'}) t] \times \langle \psi_{Ns} | \psi(0) \rangle \langle \psi(0) | \psi_{N's'} \rangle | \psi_{Ns} \rangle \langle \psi_{N's'} |. \quad (\text{A16})$$

For instance, if the atomic oscillator is initially in the ground state $|0\rangle_b$ and the field is in the Fock state $|N\rangle_a$, the density matrix reduces to

$$\rho(t) = \sum_{s=0}^N \sum_{s'=0}^N \exp[-i(\lambda_{Ns} - \lambda_{N's'}) t] d_0^{Ns} d_0^{N's'} | \psi_{Ns} \rangle \langle \psi_{N's'} |, \quad (\text{A17})$$

in terms of the expansion coefficients d_n^{Ns} defined in Eq. (4). (This expression is explicitly N -dependent, as expected.) Hence

$$\langle \psi_{Ml} | \rho(t) | \psi_{M'l'} \rangle = \exp[-i(\lambda_{Ml} - \lambda_{M'l'}) t] d_0^{Ml} d_0^{M'l'} \delta_{MN} \delta_{NM'}. \quad (\text{A18})$$

It is evident that $\rho(t)$ is effectively an $(N+1)$ -dimensional diagonal matrix in this case.

For an initial state $|(\alpha, m); 0\rangle$ we find, using Eq. (A16),

$$\rho(t) = \frac{e^{-\nu}}{m! L_m(-\nu)} \sum_{N=m}^{\infty} \sum_{s=0}^N \sum_{N'=m}^{\infty} \sum_{s'=0}^{N'} \frac{\sqrt{N! N'!} (\alpha)^{N-m} (\alpha^*)^{N'-m}}{(N-m)! (N'-m)!} \times \exp[-i(\lambda_{Ns} - \lambda_{N's'}) t] d_0^{Ns} d_0^{N's'} | \psi_{Ns} \rangle \langle \psi_{N's'} |, \quad (\text{A19})$$

where we have used the expansion of the PACS $|\alpha, m\rangle$ in the Fock basis. The corresponding matrix elements of the density matrix are given by

$$\langle \psi_{Ml} | \rho(t) | \psi_{M'l'} \rangle = \frac{e^{-\nu}}{m! L_m(-\nu)} \frac{\sqrt{M! M'!} (\alpha)^{M-m} (\alpha^*)^{M'-m}}{(M-m)! (M'-m)!} \times \exp[-i(\lambda_{Ml} - \lambda_{M'l'}) t] d_0^{Ml} d_0^{M'l'}. \quad (\text{A20})$$

Here, and in the rest of this Appendix, it is understood that contributions from terms of the form $1/(-n)!$, where n is a positive integer, vanish.

The expectation values and higher moments of the quadrature variables $\xi(t)$ and $\eta(t)$, defined in Eq. (12), can now be obtained numerically, using the above expressions for the density matrix and the matrix elements of the operators a and b in the basis $|\psi_{Ns}\rangle$. The latter are given by

$$\langle \psi_{Ns} | a | \psi_{N's'} \rangle = \sum_{n=0}^{N'} (N' - n)^{1/2} d_n^{Ns} d_n^{N's'} \delta_{N, N'-1} \quad (\text{A21})$$

and

$$\langle \psi_{N_s} | b | \psi_{N's'} \rangle = \sum_{n=1}^{N'} n^{1/2} d_{n-1}^{N_s} d_n^{N's'} \delta_{N, N'-1}, \quad (\text{A22})$$

respectively. As these are purely off-diagonal, and $\rho(t)$ is diagonal for an initial state that is a direct product of Fock states, it follows that all the odd moments of ξ and η vanish identically for all t , as asserted in the text. This is no longer true for the other classes of initial states considered.

The time-dependent reduced density matrices $\rho_k(t)$ ($k = a, b$) are given by

$$\begin{aligned} \rho_a(t) &= \text{Tr}_b [\rho(t)] = \sum_{n=0}^{\infty} {}_b \langle n | \rho(t) | n \rangle_b, \\ \rho_b(t) &= \text{Tr}_a [\rho(t)] = \sum_{n=0}^{\infty} {}_a \langle n | \rho(t) | n \rangle_a. \end{aligned} \quad (\text{A23})$$

Corresponding to an initial state $|N; 0\rangle$, these reduced density matrices $\rho_k(t)$ take the form

$$\begin{aligned} \rho_a(t) &= \sum_{n=0}^N \sum_{s=0}^N \sum_{s'=0}^N \exp[-i(\lambda_{N_s} - \lambda_{N's'}) t] \\ &\quad \times d_0^{N_s} d_0^{N's'} d_n^{N_s} d_n^{N's'} |(N-n)\rangle_a {}_a \langle (N-n)| \end{aligned} \quad (\text{A24})$$

and

$$\begin{aligned} \rho_b(t) &= \sum_{n=0}^N \sum_{s=0}^N \sum_{s'=0}^N \exp[-i(\lambda_{N_s} - \lambda_{N's'}) t] \\ &\quad \times d_0^{N_s} d_0^{N's'} d_{N-n}^{N_s} d_{N-n}^{N's'} |(N-n)\rangle_b {}_b \langle (N-n)|. \end{aligned} \quad (\text{A25})$$

Hence we have, in the Fock basis,

$${}_a \langle n | \rho_a(t) | n' \rangle_a = \sum_{s=0}^N \sum_{s'=0}^N \exp[-i(\lambda_{N_s} - \lambda_{N's'}) t] d_0^{N_s} d_0^{N's'} d_{N-n}^{N_s} d_{N-n'}^{N's'} \delta_{nn'} \quad (\text{A26})$$

and

$${}_b \langle n | \rho_b(t) | n' \rangle_b = \sum_{s=0}^N \sum_{s'=0}^N \exp[-i(\lambda_{N_s} - \lambda_{N's'}) t] d_0^{N_s} d_0^{N's'} d_n^{N_s} d_{n'}^{N's'} \delta_{nn'}. \quad (\text{A27})$$

As before, these are explicitly N -dependent finite-dimensional matrices.

For an initial state $|(\alpha, m); 0\rangle$ the expressions for $\rho_k(t)$ are given by

$$\begin{aligned} \rho_a(t) &= \frac{e^{-\nu}}{m!L_m(-\nu)} \sum_{n=0}^{\infty} \sum_{N=N_{\min}}^{\infty} \sum_{s=0}^N \sum_{N'=N_{\min}}^{\infty} \sum_{s'=0}^{N'} \frac{\sqrt{N!N'!} (\alpha)^{N-m} (\alpha^*)^{N'-m}}{(N-m)!(N'-m)!} \\ &\times \exp[-i(\lambda_{Ns} - \lambda_{N's'}) t] d_0^{Ns} d_0^{N's'} d_n^{Ns} d_n^{N's'} |(N-n)\rangle_a \langle(N'-n)| \end{aligned} \quad (\text{A28})$$

and

$$\begin{aligned} \rho_b(t) &= \frac{e^{-\nu}}{m!L_m(-\nu)} \sum_{n=0}^{\infty} \sum_{N=N_{\min}}^{\infty} \sum_{s=0}^N \sum_{N'=N_{\min}}^{\infty} \sum_{s'=0}^{N'} \frac{\sqrt{N!N'!} (\alpha)^{N-m} (\alpha^*)^{N'-m}}{(N-m)!(N'-m)!} \\ &\times \exp[-i(\lambda_{Ns} - \lambda_{N's'}) t] d_0^{Ns} d_0^{N's'} d_{N-n}^{Ns} d_{N'-n}^{N's'} |(N-n)\rangle_b \langle(N'-n)|, \end{aligned} \quad (\text{A29})$$

where $N_{\min} = \max(n, m)$. These are infinite-dimensional matrices. The corresponding matrix elements of $\rho_k(t)$ in the Fock basis are given by

$$\begin{aligned} {}_a\langle l | \rho_a(t) | l' \rangle_a &= \frac{e^{-\nu}}{m!L_m(-\nu)} \sum_{n_{\min}}^{\infty} \sum_{s=0}^{n+l} \sum_{s'=0}^{n+l'} \frac{\sqrt{(n+l)!(n+l')!} (\alpha)^{n+l-m} (\alpha^*)^{n+l'-m}}{(n+l-m)!(n+l'-m)!} \\ &\times \exp[-i(\lambda_{(n+l)s} - \lambda_{(n+l')s'}) t] d_0^{(n+l)s} d_0^{(n+l')s'} d_n^{(n+l)s} d_n^{(n+l')s'} \end{aligned} \quad (\text{A30})$$

and

$$\begin{aligned} {}_b\langle l | \rho_b(t) | l' \rangle_b &= \frac{e^{-\nu}}{m!L_m(-\nu)} \sum_{n_{\min}}^{\infty} \sum_{s=0}^{n+l} \sum_{s'=0}^{n+l'} \frac{\sqrt{(n+l)!(n+l')!} (\alpha)^{n+l-m} (\alpha^*)^{n+l'-m}}{(n+l-m)!(n+l'-m)!} \\ &\times \exp[-i(\lambda_{Ns} - \lambda_{N's'}) t] d_0^{(n+l)s} d_0^{(n+l')s'} d_l^{(n+l)s} d_l^{(n+l')s'}, \end{aligned} \quad (\text{A31})$$

where $n_{\min} = \max(m-l, m-l')$. The corresponding expressions in the case of an initial state $|\alpha; 0\rangle$ are obtained from the above by simply setting $m = 0$.

All the reduced density matrices (with elements given by Eqs. (A26), (A27), (A30) and (A31)) are hermitian. They are diagonalised numerically, and their eigenvalues are used to compute the entropies $S_k(t)$ and $\delta_k(t)$ given by Eqs. (10). In the case of infinite-dimensional matrices, rapid convergence in numerical computation is provided by the factorials in the denominators of the summands in the expressions derived above for the matrix elements.

We use double precision arithmetic with an accuracy of 1 part in 10^6 . As mentioned in the text, we use the equality of $S_a(t)$ and $S_b(t)$, and the condition $\rho^2(t) = \rho(t)$ for the density matrix of the total system, as some of the checks on the numerical computations, as we are only dealing with pure states.

-
- [1] See, for instance, R. W. Robinett, Phys. Rep. **392**, 1 (2004).
 - [2] K. Tara, G. S. Agarwal and S. Chaturvedi, Phys. Rev. A **47**, 5024 (1993).
 - [3] C. Sudheesh, S. Lakshmibala and V. Balakrishnan, Phys. Lett. A **329**, 14 (2004).
 - [4] C. Sudheesh, S. Lakshmibala and V. Balakrishnan, Europhys. Lett. **71**, 744 (2005).
 - [5] C. Sudheesh, S. Lakshmibala and V. Balakrishnan, J. Opt. B: Quant. Semiclass. Opt. **7**, S728 (2005).
 - [6] G. S. Agarwal and K. Tara, Phys. Rev. A **43**, 492 (1991).
 - [7] S. J. van Enk, Phys. Rev. Lett. **91**, 017902 (2003); for a discussion on the decoherence of entanglement, see also S. J. van Enk, Phys. Rev. A **72**, 022308, (2005).
 - [8] I. Sanz, R. M. Angelo and K. Furuya, J. Phys. A: Math. Gen. **36**, 9737 (2003).
 - [9] G. S. Agarwal and R. R. Puri, Phys. Rev. **A39**, 2969 (1989).
 - [10] A. Zavatta, S. Viciani and M. Bellini, Science **306**, 660 (2004).
 - [11] W. H. Press, S. A. Teukolsky, W. T. Vetterling and B. P. Flannery, *Numerical Recipes in C*, Cambridge University Press, Cambridge, 2001, pp. 475-481.
 - [12] M. Galassi, J. Davies, J. Theiler, B. Gough, G. Jungman, M. Booth and F. Rossi, *GNU Scientific Library*, GNU Software, 2005.
 - [13] That the revival time is inversely proportional to the coefficient of the term in the Hamiltonian that is quadratic in the quantum numbers concerned is a general feature. See S. Seshadri, S. Lakshmibala and V. Balakrishnan, J. Stat. Phys. **101**, 213 (2000).
 - [14] A quantitative measure of entanglement is provided by the logarithm of the trace norm of the reduced density matrix (see G. Vidal and R. F. Werner, Phys. Rev. A **65**, 032314 (2002)). This is also the measure of entanglement used, for instance, in Ref. [7].
 - [15] S. D. Du and C.-D. Gong, Phys. Rev. A **48**, 2198 (1993).
 - [16] C. Sudheesh, *Non-classical effects in wave packet dynamics*, Thesis, Indian Institute of Technology Madras (unpublished), (2005).